

Improved Melting Process in Cupola Furnace and Production Loss Reduction with Incinerator-Melt Framework

Huzifa A. Fidvi and Akash M. Langde

Anjuman College of Engineering and Technology, Mangalwari Bazaar Road, Sadar, 440001 Nagpur, India

Key words: Cupola furnace, incinerator-melt enhancement framework, thaw-degree perusal model, O₂-Scurtinizer model, Kiln Flicker Espial Technique

Abstract: In the cupola process, the key operational goals are to keep the iron properties within the specified limits and to maintain the required production rate. However, over the years it has not improved significantly and always relied on melting processes and loss of productivity. Therefore, it efficiently proposed a novel Incinerator-Melt Enhancement Framework which addresses the challenges in melting processes and loss of productivity. This framework introduced a Thaw-Degree perusal model it scrutinizes the melting rate based on the selection of optimum input parameters that enhance the melting process. In addition, an effective controller design O₂-Scurtinizer model is used to regulate the O₂ that integrates simple step-response testing and nonlinear optimization. Moreover, to handle fluctuations, it implements the Kiln Flicker Espial Technique to judge the stability of the furnace using the dynamic sampling method. Finally, the proposed system effectively enhances the melting process and the effects of variations in the air constituents resulting in better melting performance and reduced loss of production.

Corresponding Author:

Huzifa A. Fidvi

*Anjuman College of Engineering and Technology,
Mangalwari Bazaar Road, Sadar, 440001 Nagpur, India*

Page No.: 3793-3804

Volume: 15, Issue 24, 2020

ISSN: 1816-949x

Journal of Engineering and Applied Sciences

Copy Right: Medwell Publications

INTRODUCTION

One of the world economy's fundamental industries is ferrous metallurgy. This covers such measures as natural resource mining, enrichment, burning, cast iron and steel production, etc.^[1]. Cast iron smelting is one of the most complex steps in the processing of raw material steel. A cupola furnace is a small explosive oven about one order in size. It is used in cast iron production and is used particularly in the decrease of minerals^[2]. Usually, pig iron, steel scrap and limited amounts of flux (quiet stone) and coke are included. The loading is not reduced in the couple; the load is instead oxidized and some of the silicon (as SiO₂),

manganese (as MnO) and iron (as FeO) move through the slag the loading is not reduced^[3]. The CO and CO₂ in the pumped air coke.

The cupola uses less coke than the explosive furnace and the CO₂ in the gases normally reaches CO. In comparison to the blast furnace, depending on the circumstances when cast iron moldings are ready for casting the coupe furnace operates intermittently^[4]. By way of control steps to stabilize key parameters, control of the melting process is minimized. For starters, the iron content in the charger sets the overall demand for heat smelt and affects the reduction of oxide, gas dynamics and many other furnace processes^[5]. The coke strength and the fraction content help to conserve coke and

improve output efficiency. Theoretical combustion temperature increases as the oxygen content of the explosion increases, the limiting temperature of the heat exchange areas decreases and the temperature of the explosive oven gas decay. Blast heat furnace affects cast iron consistency, the productivity of furnace, smelting rate, etc.^[6]. Therefore, the thermal environment should be maintained under such limits to prevent overheating or overcooling of the oven as this could lead to an irregular operation. The thermal condition of the burning process is estimated by the chemical composition of cast iron and slag after tapping in current blowing oven technology which ensures that the modification of control measures is considerably overdue^[7]. In this respect, ferrous metallurgy specialists have a very demanding role, including the chemical composition of cast iron and slag during tapping in predicting the changes in the thermal condition of the blast furnace^[8].

In research works, by foreign and Russian scholars this problem can be solved by various approaches. While the challenge is widespread, it is not fully solved and is important to modern production^[9]. The research papers will most frequently identify the methods used to calculate silicon content forecast values in cast iron and cast iron temperatures. There is also a desire to use machine learning algorithms for calculating forecast values^[10]. The works suggest that such a thermal state as titanium element be taken into account. This metric considers the balance between the titanium substance in cast iron and slag, complementing existing methods of determining the thermal condition.

A comparative analysis of blast furnace indicators and operating parameters is not always useful in detecting the relationship between cause and effect and in drawing firm conclusions about the reasons for variations. This is attributed to the incompleteness of the documents used and the numerous inaccuracies found in it as well as the accounting imperfection along with the lack of research into specific factors^[11]. In this connection, the problem of simulation also proves its relevance under the modern conditions of production. Melting efficiency enhancement is one of the primary objectives of the blast-furnace melting process. The operator while being able to predict the furnace behavior during different control activities, can bring the furnace to a more productive operating mode with lower coke output^[12]. So let's remember two relevant issues for cupola furnace operators-the improved efficiency in iron melting and reduced coke consumption. One of the parameters which affect the considered technical and economic performance is the content of iron in the charge^[13]. Iron content in the charge not only stipulates the overall demand for melting heat but also influences the reduction of oxides, gas dynamics and a variety of other processes in the furnace. At the same time, the regulation of blast parameters such as

oxygenation, humidification and blast heating, also has a major and rapid effect on the production and coke consumption^[14]. This is related to the fact that the enrichment of oxygen favors indirect iron reduction conditioned by the increased concentration of the reduction components in the tuyser gas.

While its temperature is higher, oxygen enrichment contributes to a higher coke yield, despite an increased indirect decrease. This is because the heat release of coke carbon is greatly diminished by the decreased real blow rate^[15]. Compared to low explosion temperatures, the furnace performance gain in these alternatives is relatively lower. When adding natural gas during oxygen enrichment the maximum production gain is demonstrated at a set blast temperature. The inclusion of natural gas and the respective rise in the indirect reduction in coke saving in this alternative. Continuous assessment of the controlled parameters is important to monitor the blast furnace operation effectively. In automatic control systems and decision support systems, the information is stored and used. All this leads to a low-cost efficiency of melt output and temperature overheating^[16].

From the above discussion, it is perceived that there is a great need to develop new technology for the enhancement of a cupola furnace.

Literature review: Pribulova *et al.*^[17] proposed that specific information should be given concerning the production of slage in a cupola furnace, its chemical structure and current possible uses and addresses the land, especially in respect of the use of slag in the building industry which plays an important role. In the development of concrete made from slag alone, the writers used air-cooled and granulated slaughter from cupola furnaces. The use of granulated slag from cupola furnaces in cement-free concrete as a substitute for the granulated blast-furnace slag has not proved effective.

Elorz *et al.*^[1] proposed the method of production of cast iron in cupola furnace, the main type of oven used when the engineered material is made is mentioned there. Various solved questions surrounding mass and energy balance can better explain the production of cast iron. This chapter also discusses the value of raw materials, since, optimization challenges are posed through the use of the raw materials. Also included are the solved problems of sweetening and dephosphorization.

Gabra *et al.*^[18] this work try to address the issue by proposing and analyzing a way of reducing coke consumption in a foundry cupola studied by hybridizing it with biomass wood gasifiers. Wood fuel is very cheap and readily available. The blast air flowing through a few furnaces can be ignited using a gasifier that can be used to burn. The chemistry in the various stages of the cupola furnace and reasons for that huge percentage of heat energy loss during the melting process was properly discussed.

Kavousi-Fard *et al.*^[19] deal with core issues of achieving productive process models and optimizing controls. The new predictive approach is built-in Electro-Arch Furnaces (EAFs) to increase VAR (SVC) static efficiency. Thus, a new nonparametric approach is being built to build forecast intervals (PIs) around reactive energy consumption trends in the SVC based on the Lower Upper Bound Estimation process (LUBE) and Supporting Vector control (SVR). The suggested approach uses the PI principle to model reactive power uncertainties, thereby avoiding flickering problems.

Meier *et al.*^[20] discussed an Electric Arc Furnace (EAF) dynamic process simulation model through the improvement of heat transfer modeling and simulations, particularly through the radiation system within the EAF. Modeling and simulation for the heat transfer within the EAF are enhanced by the inclusion of the electrode within the models, for instance by modeling the electrode surfaces as a radiative surface concerning convective and radiative heat transfer to and from electrodes.

Elkoumy *et al.*^[21] involved the development of a guide for the compositional changes in steel melting at the grinding stage of the Electric Arc Furnace (EAF). The model is built on actual calculations compared with thermodynamic forecasts. The parameters analyzed are the carbon and temperature content of steel melting. These measures are equipped with simple regression equations and contour plots for the best control of the stages to be made.

Pribulova *et al.*^[17] resulted in lack of transparency and comprehensibility^[1] reported energy losses during the process steps represent inefficiencies that waste energy

and increase the costs of melting operations and in^[17] the number of model parameters comparatively high and the negative effect of measuring noise must be determined when the model forecast is high. Further Kavousi-Fard *et al.*^[19] problems of achieving efficient model processes and maximizing power were not answered. Meier *et al.*^[20] furnace conditions could not be judged by the operator in time, many raw materials were to be lost in^[21] problems include data expertise, lack of uniform furnace conditions metrics.

Therefore, from the above-mentioned issues, there is a greater more need to develop a novel method to enhance the melting performance and reduced productivity loss of cupola furnace.

Advancement in melting process and efficiency of cupola furnace:

A cupola furnace is a small explosive furnace used in cast iron and used in mining ores in particular (Fig. 1). Melting rate, the effect of air materials, fuel consumption and volume of CO₂ released from the cupola furnace are important concerns for reducing the melting process and loss of productivity in cupola furnaces. Among which the melting rate is the initial consideration which is reflected in the furnace output. Many factors reduce the melting rate, so, analysis of the melting rate based on optimal input parameters is important. Existing work for enriching the melting rate resulted in an error due to inconsistent and nonlinear selection of input parameters. Although, the effect of air constituents on the metal occurs increasing the melting rate, this could lead to increased gas formation. Prevailing control strategies use a set point control feature that resulted in limited effectiveness and difficulty faced. A

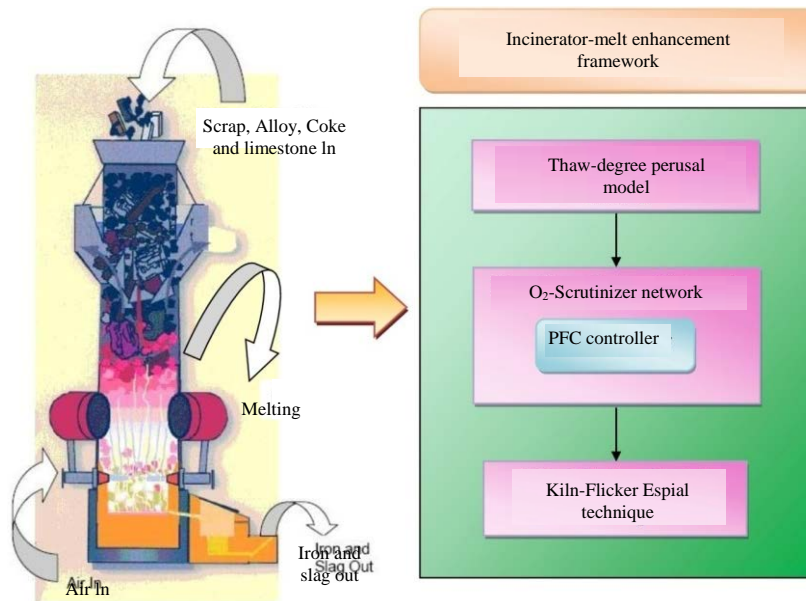


Fig. 1: Incinerator-melt enhancement framework

control strategy for controlling and regulating the paramount constituent of air is to be established based on this. The overall output and average cost relays, besides, the volume of fuel used by the cupola furnace. Incorrect management of time variability can also cause furnace failure that leads to lower performance, higher fuel consumption and extreme production and operational aftermath. Also, previous methods failed to evaluate variations that are responsible for operational efficiency. Therefore, the work introduced a novel incinerator-melt enhancement framework that concerns the challenges in the melting process and productivity loss. Figure 1 shows the block diagram of the proposed framework.

In the framework, a Thaw-Degree perusal model for scrutinizing the melting rate is suggested based on selecting optimal input parameters which enhances the melting process. This model is formulated whereby statistically significant links between the control variables and the rate of iron melting is defined. Furthermore, the major constituent O₂ is to be monitored and regulated by using an efficient controller-model design. In order to achieve this O₂-the Scrutinizer model is hosted which involves simple, nonlinear optimization and step-response test. In addition, the operator must correctly determine the furnace condition and then take the steps of improvement based on the condition that the fuel consumption can be reduced. In order to handle fluctuations, the framework implements Kiln Flicker Espial technology for determining the furnace's stability. The highest fluctuation identification rate among the other methods is this method which has considerable dominance in class imbalance issues. The melting rate in the cupola furnace is initially analyzed with the perusal model of the thaw degree is described below.

MATERIALS AND METHODS

Thaw degree perusal model: The thaw degree perusal model is expected to be associated with other control variables for the melting phase. To check the existence of connexion between variables, designing statistic models such as the thaw grade perusal model can be used. Thus, the technical solution followed requires two main phases. First, the generation of a multi-thaw perusal model represents the predicted relationships between the iron melting rate and the independent variables (air blast pressure, melting time and fuel consumption). Secondly, the validity and appropriateness of these models were tested using statistical tools such as hypothesis testing, variance analysis (ANOVA), determination coefficient and R². A response variable (Y) is connected to a set of control variables, as shown in the Thaw degree perusal model provided by Eq. 1. In the development of a thaw perusal model, it is important to test the parameters such as the intercept and regression coefficients correlated with control variables:

$$X = p_0 + p_1 y_1 + p_2 y_2 + p_3 y_3 + \dots + p_k y_k + \epsilon \quad (1)$$

where, X-is a k control variable function that is an error word. The model's interception of p₀ is and the control coefficients y₁, y₂ and y₃ of p₁, p₂, p₃ are respectively regression coefficients. With the q₀, q₁, q₂, q_k coefficients, the corresponding solution variable X can be calculated by using the sample data shown in Eq. 2 with its control variable y₁, y₂, ..., y₂ model parameters:

$$X = q_0 + q_1 y_1 + q_2 y_2 + q_3 y_3 + \dots + q_k y_k + \epsilon \quad (2)$$

Where:

- q₀ = The model intercept
- q₁ = The control variable
- y₁ = Coefficient of regression
- q₂ = The control variable
- y₂ = Associated regression coefficients
- q₃ = The control variable
- y₃ = Assigned regression coefficient

The differing selection for the melting rate process is explained in the next section.

Variables selection: Both independent variables are taken from the relation between a dependent variable, air explosion pressure (P), melting time (T) and ingested fuel (F). These variables have the following measurement unit definitions; the blasted air pressure is the blower air pressure given in bar; the melting time (T) is the melting time of metals within minutes; fuel consumed (F) is the fuel consumed by the melting of metals within kilograms and the measurement of the melting rate (M). The above considerations have been selected from the iron fusion rate control variables.

Rational effect on the melting point of those conditions. A rise in air pressure, for example, raises the airspeed of the pipe and thereby raises the melting rate of iron in contact with solid fuel.

Logically, the melting rate in kg min⁻¹ would change if the volume of iron per unit of time is increased. The diagrams of scattering were used to verify the initial set of control variables to explain the existence of such informative relationships between these factors. Below are the mathematical parameters for the melting stage relationships.

Assumptions of models: The numerical assumptions are given below: the relationship between the melting rate and its associated control variables was predictable (application of scatter diagram).

There is no multi-linearity between cold, melting and fuel consumption. Random errors (o) are distinct and usually dispersed with constant variance and average zero. Formulation of multiple thaw degree perusal model with the formulation of models and testing of hypothesized coefficients are listed below.

Models formulation: A cupola furnace using carbon as energy was designed based on models assumptions and selected variables for the following Thaw grade model perusal.

Model: The furnace is used as fuel for a cupola:

$$\text{Exp (M/P, T, F)} = q_{0cf} + q_{1cf}P + q_{2cf}T + q_{3cf}F \quad (3)$$

Where:

- Exp (M/P, T, F) = The anticipated melting rate value in kg/min because of the different P, T and F variables
- q_{0cf} = Model interception
- q_{1cf} = The coefficient of regression consistent with the model air pressure
- q_{2cf} = Coefficient of regression compared to the sample melting period
- q_{3cf} = The coefficient of regression consistent with model fuel consumption

The following section explains the testing model validity of the hypothesis.

Hypothesis: Test of the validity of the model and individual evaluation of multi-thaw perusal model coefficients.

Model hypothesis 1: For a cupola furnace using ? as fuel is presented as in Eq. 4:

$$H_0 : \beta_{icf} = 0, j = 1, 2, 3 \quad (4)$$

If H_0 is rejected, then H_1 : at least one $\beta_{icf} \neq 0$. Specific coefficient analyses of the perusal models of multiple thaw degree hypothesis II were provided with every independent variable in Eq. 5:

$$H_0 : \beta_{1-3cf} = 0 \text{ vs } H_1 : \beta_{1-3cf} \neq 0 \text{ for the model} \quad (5)$$

The null hypothesis is predicated on the assumption of a not statistically relevant relationship between the melting rate and the blast strain, the melting time and the consumed fuel. In addition, the main constituent O_2 should be controlled and regulated using an effective controller-model system as set out below.

O_2 -Scrutinizer model: O_2 -Scrutinizer model helps regulate and track the contents of oxygen in the cupola furnace. To better understand process dynamics a divided approach is applied using step-response simulation and non-linear optimization with a neural backpropagation network (BPNN). The architecture of the PFC controller is based on control theory, due to this structure. The way is thought about:

$$A_m(k) = A_l(k) + A_{nl}(k) \quad (6)$$

where $A_l(k)$ is the output of the step-response model, $A_{nl}(k)$ is the Non-linear component accomplished by error reduction among $A_l(k)$ and $A(k)_i$, ($i = 1, 2, \dots, N$). $A(k)_i$, ($i = 1, 2, \dots, N$) is the value of the process output $A(k)$ of group I, N is defined as the process category total amount.

The basic modeling theory is that the process model must be as accurate as possible for optimal results for the subsequent controller configuration. In this context, the mathematical model represents the dynamics of the mechanism as near as possible. This shows that there may not be a minimum difference between the estimated model output and the real process output. Below is the phase reaction model for the widespread method.

Generalized process model for step-response: The Field Control Station (FCS) is designed to read and model the answers to real-time processes by linking to the oxygen material control loop. Figure 2 displays the phase test settings and the time to analyses is 5s.

The input is the PID's set-point for oxygen content. In Fig. 2, the input is changed to get the response of the generalized process from 4.5-5%. Using the modeling method proposed:

$$A_l(k) = a_1A(k-1) + b_1u(k-5) \quad (7)$$

The widespread method is eventually accomplished by optimizing BPNN:

$$A_m(k) = A_l(k) + A_{nl}(k) = a_1A(k-1) + b_1u(k-5) + g \left(\sum_{i=1}^7 w3(i) g \left(\sum_{j=1}^4 w2(k-j) + w2(i,d+1)y(k-1) \right) \right) \quad (8)$$

The above-mentioned modeling consists of the combination of a first-order plus a linear term model (FOPDT) with a nonlinear optimization residual model. The FOPDT will catch the key characteristic of this method. A careful model should first be defined, before more nonlinear optimization, when considering other implementations which can capture the principal process function and cannot be limited to FOPDT. The following section discusses the concept of modeling errors in the algorithm modeling method.

Modeling algorithm: For the step-response model, denote $A(v)$, $A(\infty)$, U_0 the continuous value of the measured process output and the input phase signal amplitude as the measured process output. Then measures the operation gain with $K = A(\infty)/U_0$.

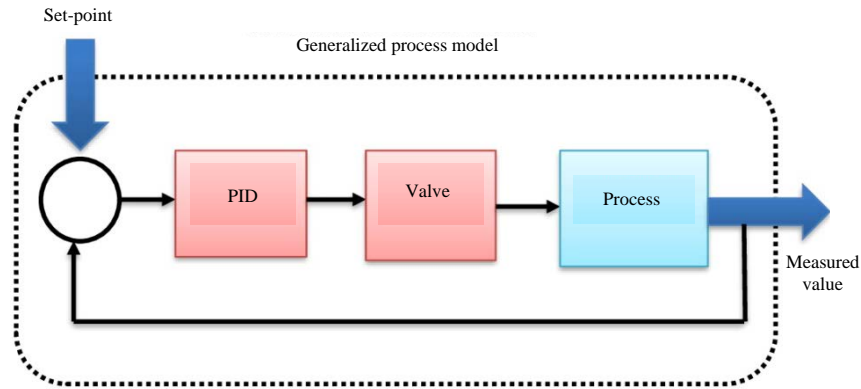


Fig. 2: Generalized process model input-output

The required model order should be determined first and that in compliance with the case study the common first order plus dead period model will be implemented:

$$D(s) = \frac{Ke^{-ts}}{Ts+1} \quad (9)$$

The calculated output $A(t)$ is convertible into $A^*(v) = A(t)/A(\infty)$ and:

$$A^*(v) = \begin{cases} 0 & t < \tau \\ 1 - e^{-\frac{t-\tau}{T}} & t \geq \tau \end{cases} \quad (10)$$

Two-time points $A^*(v_1) = 0.39$, $A^*(v_2) = 0.63$ are determined to obtain T and τ as follows:

$$\begin{aligned} T &= 2(v_2 - v_1) \\ \tau &= 2v_1 - v_2 \end{aligned} \quad (11)$$

The discrete form $A_i(k)$ in Eq. 6 can be obtained after using the sampling time T_s . The nonlinear part $A_{nl}(k)$ in Eq. 6 is achieved as follows. First define the modeling error as:

$$\bar{e}(i) = A(k)|_i - A_{ii}(k), (i=1,2,\dots,N)$$

where $A_{ii}(k)$, ($i = 1, 2, \dots, N$) the value of $A_i(k)$ group i . By minimizing $\sum \bar{e}(i)$, ($i = 1, 2, \dots, N$) through a BPNN, the following model will be obtained:

$$A_{nl}(k) = g \left(\sum_{i=1}^I w_3(i) g \left(\sum_{j=1}^d w_2(i,j) u(k-j) + \sum_{j=1}^d w_2(i,d+1) y(k-1) \right) \right) \quad (12)$$

where $w_2(i, j)$, $w_3(i)$ are the weights between BPNN layers, I are the output nodes number. In this case, it took the full delay into account $d = \tau/T_s$ that can be estimated

through the step-response test in Eq. 7 and $g(x)$ is the activation function adopted as $g(x) = 1/(1+e^{-x})$. Further, define $nl(k) = A_{nl}(k)$ Eq. 6 is discretized and rewritten as:

$$A_m(k) = a_1 A_m(k-1) + b_0 u(k-d-1) + nl(k) \quad (13)$$

The PFC controller system design predicted output result is followed below with the three constructed parts.

Control system design: Equation performance estimation (Eq. 13) will be processed as data of gradual systems. Control system architecture by adding $\Delta = 1-z^{-1}$ which results as follows:

$$\begin{aligned} A_m(k) &= R_1 A_m(k-1) + R_2 A_m(k-2) + \\ &B_{1,0} \Delta u(k-d-1) + \Delta nl(k) \end{aligned} \quad (14)$$

where, $R_1 = 1+a_1$, $R_2 = -a_1$, $B1, 0 = b_0$. The future step-away process performance forecast is built in three sections for the comfort of the subsequent PFC design, i.e., $A_{past}(k+d+p)$ that is known at present and related to past process inputs and outputs measured values through (Eq. 7), G_p , U_p is unclear but connected to current and future process inputs and the forecast error, all the nonlinear dynamic component denoted as $\Delta_{nl}(k+p)$ and the feedback correction part denoted as $A(k) - \hat{A}(k)$. Now, the future output prediction is formulated as:

$$\begin{aligned} \hat{A}(k+d+p/k) &= A_{past}(k+d+p) + G_p U_p + \\ \Delta nl(k+d+p) &+ (A(k) - \hat{A}(k)) (p=1,2,\dots,N_y) \end{aligned} \quad (15)$$

where, N_y is the prediction horizon and:

$$U_p = [\Delta u(k), \Delta u(k+1), \dots, \Delta u(k+p-1)]^T \quad (16)$$

$$G_p = \begin{bmatrix} B_{1,0} & & & \\ B_{2,0} & B_{1,0} & 0 & \\ \dots & \dots & & \\ B_{p,0} & B_{p-1,0} & \dots & B_{1,0} \end{bmatrix} \quad (17)$$

And:

$$\begin{aligned} B_{1,0} &= b_0 \\ B_{i,0} &= \sum_{j=1}^{i-1} R_j B_{i-j}, i=2, \dots, p \end{aligned} \quad (18)$$

Then it expressed the controller design of the PFC strategy with the combination of set-point. The control input is represented as a combination of simple set-point functions in conjunction with the PFC strategy:

$$u(k+i) = \sum \lambda_j f_j(i) \quad (19)$$

where λ_j are the $f_j(i)$ weights, at sampling time I is the basis function and M is the order of the basic functions. The setpoint A_s is further processed into the smooth monitoring set point:

$$A_{ref}(k+d) = A(k) \quad (20)$$

$$\begin{aligned} A_{ref}(k+d+p) &= \mu^p A(k) + (1+\mu^p) A_s \\ p &= 1, 2, \dots, N_A \end{aligned} \quad (21)$$

where, μ is the smoothing factor. The cost feature for PFC (15) is formulated as:

$$J = \min (A_{ref}(k+d+N_y) - \hat{A}(k+d+N_y/k))^2 \quad (22)$$

When $u(k) = u(k+1) = \dots = u(k+N_y-1)$ adopted to minimize (Eq. 22) the optimization leads to:

$$\Delta u(k) = \frac{\left(A_{ref}(k+d+N_A) - A_{past}(k+d+N_A) - \right)}{\left(\Delta nl(k+d+N_A) - A(k) + \hat{A}(k) \right)} / B_{N_A,0} \quad (23)$$

$$u(k) = \lambda_1 = u(k-1) + \Delta u(k) \quad (24)$$

Note that $\Delta nl(k+d+N_A)$ is not known, iteration is then proposed:

$$\begin{aligned} \Delta nl(k+d+N_y)^0 &= 0 \\ \Delta u(k)^0 &= \frac{\left(A_{ref}(k+d+N_A) - A_{past}(k+d+N_A) - \right)}{\left(\Delta nl(k+d+N_A)^0 - A(k) + \hat{A}(k) \right)} / B_{N_A,0} \\ \Delta nl(k+d+N_A)^{k+1} &= \Delta nl(k+d+N_A)^k + \\ \delta(k) \left(A_m^k(k+d+N_A) - \hat{y}^k(k+d+N_A) \right) \\ \Delta u(k)^{k+1} &= \frac{\left(y_{ref}(k+d+N_A) - A_{past}(k+d+N_A) - \right)}{\left(\Delta nl(k+d+N_A)^{k+1} - A(k) + \hat{A}(k) \right)} / B_{N_A,0} \end{aligned} \quad (25)$$

where, 0 is the initial value for the associated variables, subscript k is the k th iterative calculation. $y_m^k(k+d+N_A)$ and $\hat{A}^k(k+d+N_A)$ are the output prediction values obtained by substituting $\Delta u(k)^k$ into (Eq. 14) and (Eq. 15), respectively. $\delta(k) = 1/k$ is the convergence factor. If $\hat{A}^k(k+d+N_A) = A_m^k(k+d+N_A)$ is satisfied, the control law $\Delta u(k)^k$ is optimal. However, during the implementation, if the absolute error between $A_m^k(k+d+N_A)$ and $\hat{A}^{k+1}(k+d+N_A)$ is smaller than an accepted tolerance, $\Delta u(k)^k$ will be implemented as the practical control input. The model design of NPFC-PID for oxygen content is explained below with the convergent analysis.

Model design: The PID controller and the oxygen controller are considered a generalized method for the design of PFCs to allow for PID rejection of disturbances at a reasonably rapid rate. The other benefit is to use and specifically simulate valve dynamics.

Figure 3 displays a set-point order SV and the measured oxygen content PV, the control mechanism is calibrated. To make the PFC controller convergent, the analysis of convergence is explained in a subsequent section. The convergence analysis of Eq. 25 reveals that $\delta(k)$ is inversely associated with k which shows that as k increases, changes of $\Delta nl(k+d+N_A)$ and $\Delta u(k)$ decreases. Here, define $\Delta nl(k+d+N_A)$ as the actual value of $\Delta nl(k+d+N_A)^k$ and that $\hat{A}^k(k+d+N_A)$ will converge to $A_m^k(k+d+N_A)$. If $\Delta nl(k+d+N_A)$ is obtained. The work gives the conclusion below.

Theorem: For the process modeled by Eq. 1 and a PFC design by Eq. 25, adopt $\delta(k)$ to satisfy $\delta(k) \in (0, 1)$, $\lim_{k \rightarrow \infty} \delta(k) = 0$ then the PFC is convergent. Thus the oxygen content is regulated than to reduce a large amount of fuel consumption and monitoring the overall work of furnace Kiln-Flicker Espial Technique is followed below.

Kiln Flicker Espial technique feature extraction algorithm: To solve this problem, the analysis uses many approaches to test the stability of an iron furnace. Results show that the hierarchical sampling system neural networks has the highest identification rate of anomalies relative to the other methods and has a high dominance of class disparity issues.

A "relation" to quantify feature significance is established by the relief process. The correlation is a vector with an initial function of each variable. Description of association components for each function in the subset decides the importance of a subset of features. Due to the performance of Relief in many respects, relief is particularly developed for binary classification problems. The extension edition relief-F can solve multiclass problems. During these experiments, the

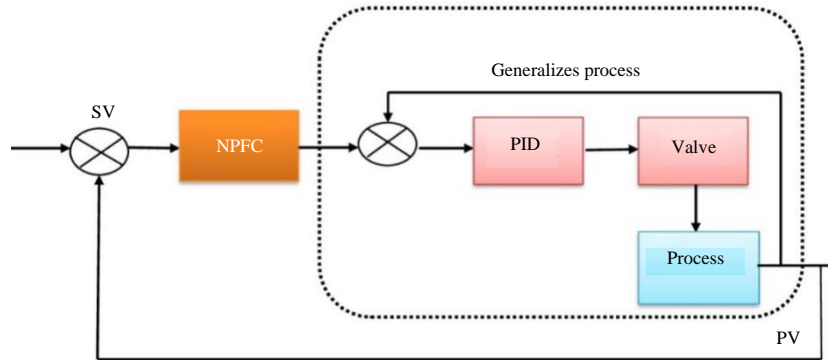


Fig. 3: NPFC-PID oxygen contents regulation block

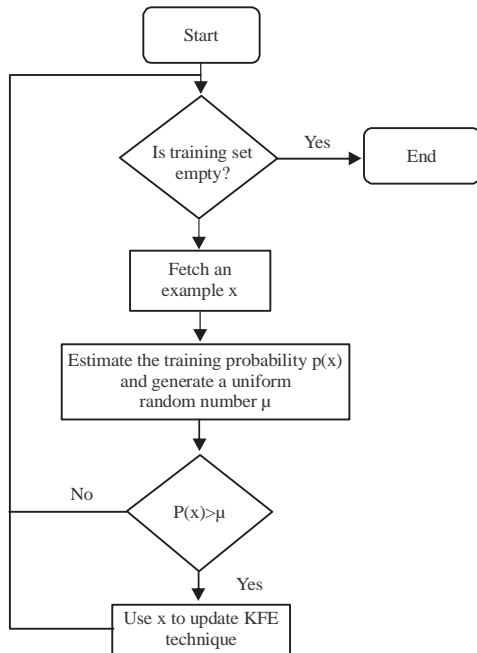


Fig. 4: Flowchart of the dynamic sampling method for the KFE technique

Classification results will be improved by the relief algorithm and if so, an adequate number of functions will be taken to maximize the performance and reliability of the classification method.

Dynamic sampling method of Kiln-Flicker Espial technique: Kiln-Flicker Espial technology has been proved to be able to study complex grading boundaries and to be used in binary classification problems directly. Therefore, the KFE technology is adopted as our basic model and a Dynamic Sampling (DyS) approach for the KFE methodology to manage class imbalance problems is developed.

The DyS-KFE Technique Algorithm displays the general flow in Fig. 4. DyS incorporates sampling and

processing techniques that transcend the drawbacks of a pretreatment procedure, in comparison to the pre-samples approaches. DyS's simple concept is to dynamically choose examples for training. It deletes some instances to prevent information loss, however, it chooses training samples dynamically to avoid repetitive information and allow the best use of the training data. The overall framework, therefore, effectively analyzes the melting rate and regulates the oxygen content in the cupola furnace, in addition to monitoring the furnace's performance and stability to reduce the loss of productivity.

The proposed model thus faces the above challenges concerning the effect on melting, air and fuel consumption, resulting in lower productivity losses and an improved melting mechanism.

RESULTS AND DISCUSSION

The proposed methodology is implemented in MATLAB and the simulation results are discussed below. The proposed technique is described in previous section 3 and in this section, the detailed explanation and its performance are analyzed:

- Platform: MATLAB
- OS: Windows 10
- Processor: Intel core i5
- RAM: 8 GB RAM

Simulation outputs: The incinerator-melt enhancement framework for cupola furnace melting rate, oxygen regulation and overall performance monitoring in the working of cupola furnace the simulation outputs are shown in Fig. 5-13.

Figure 5 states the Melting rate analysis of Original vs. Smoothened value of coefficient C1 varies with the axial length. Thaw-degree perusal model tune the parameters and analyze the melting rate performance of coefficient C1.

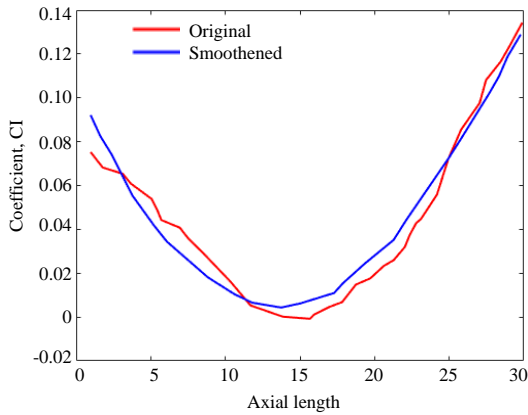


Fig. 5: Melting rate analysis of original vs. Smoothened of C1

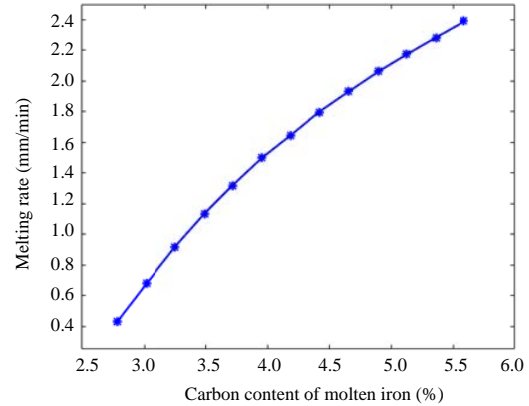


Fig. 8: Melting rate for molten iron

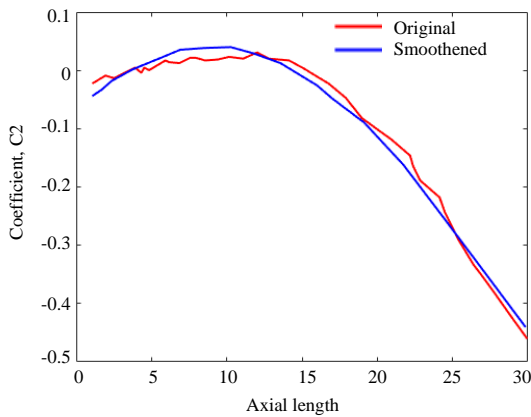


Fig. 6: Melting rate analysis of original vs. Smoothened of C2

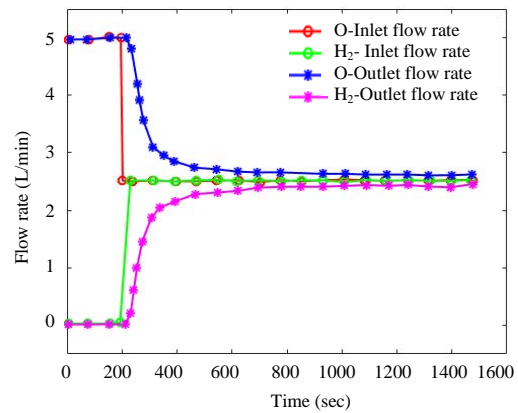


Fig. 9: Oxygen regulation flow rate of H₂ and O

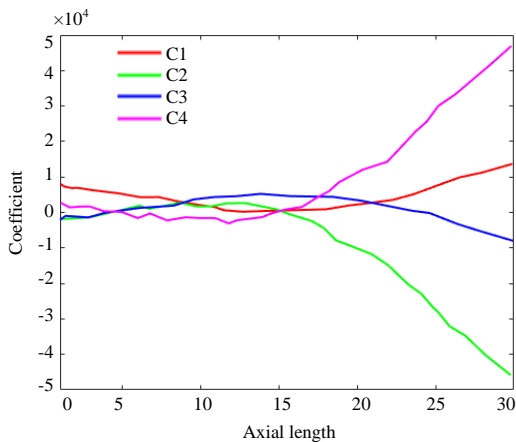


Fig. 7: Melting rate analysis of various coefficients

Figure 6 states the Melting rate analysis of Original vs. Smoothened value of coefficient C2 varies with the axial length. Thaw-degree perusal model tune the parameters

and analyze the melting rate performance of coefficient C2. Figure 7 states the Melting rate analysis with varying coefficient contrasts with the axial length. Thaw-degree perusal model tune the parameters and analyze the melting rate performance of each coefficient.

Figure 8 states the melting rate performance of molten iron. In this carbon content for each melting rate increases simultaneously it increases the melting rate with percentage.

Figure 9 shows the flow rate of H₂ and O thus it regulates the oxygen content in the cupola furnace. It estimates the oxygen inlet flow and outlet flow and also H₂ inlet flow and outlet flow with the varying time per second.

Figure 10 shows the oxygen content, airblast pressure and fuel conception for the regulation of oxygen in the cupola furnace. It tunes the parameters to increase and varying the oxygen in each time. Figure 11 states the oxygen content in the set point.

Figure 12 states the static temperature for air combustion and oxy-fuel combustion it varies the

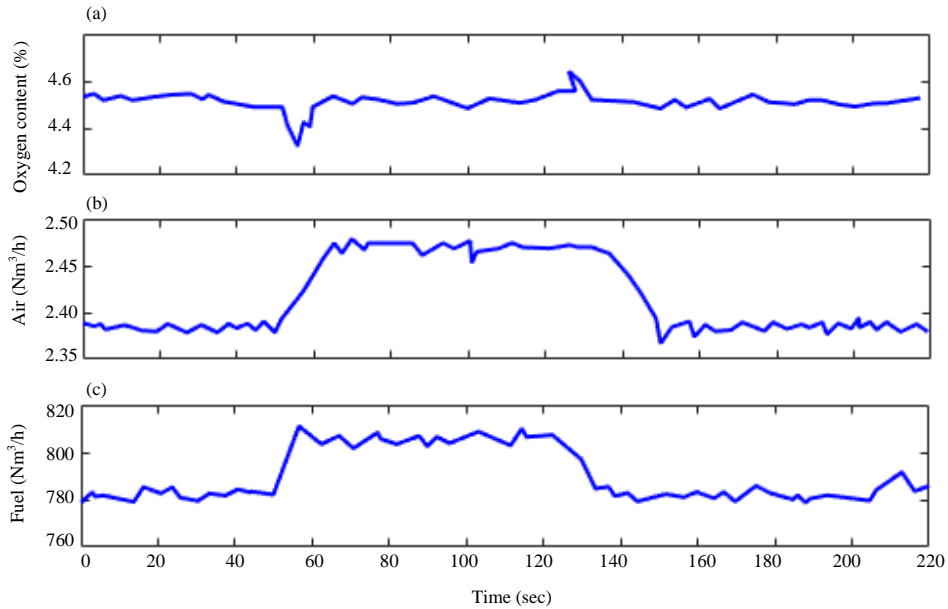


Fig. 10(a-c): Oxygen content in air, fuel

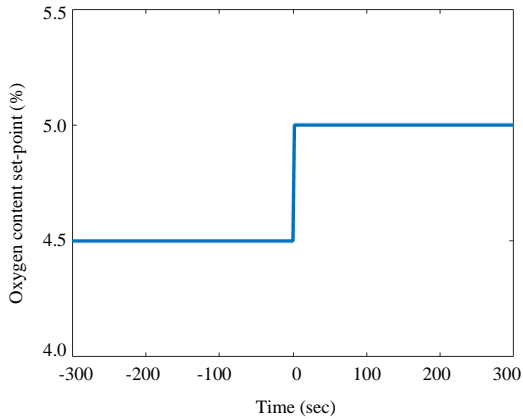


Fig. 11: Oxygen content in the set point

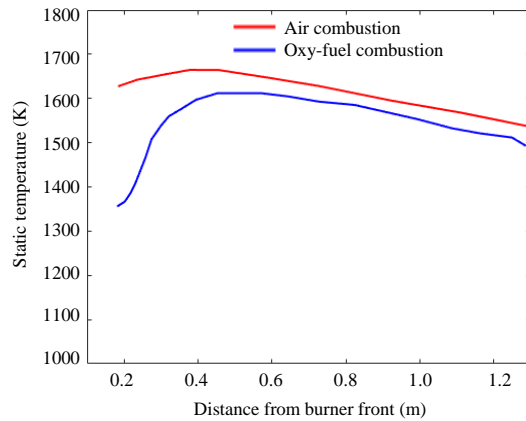


Fig. 12: Static temperature

temperature it depends on the distance between the burner and the substance. Once, the Air combustion gets increases the oxy fuel combustion gets decrease.

Figure 13 states the Furnace temperature of the cupola it monitoring the performance and the stability of the furnace.

Comparison analysis: To evaluate the overall comparison of the proposed system with an existing system, the following approaches are taken into an account such as Artificial Neural Network (ANN), Kernel principal component analysis (KPCA), Kernel fisher Discriminant analysis (KFA), Support vector machine, Predictive Functional Control (PFC) and Logistic Regression Model (LRM).

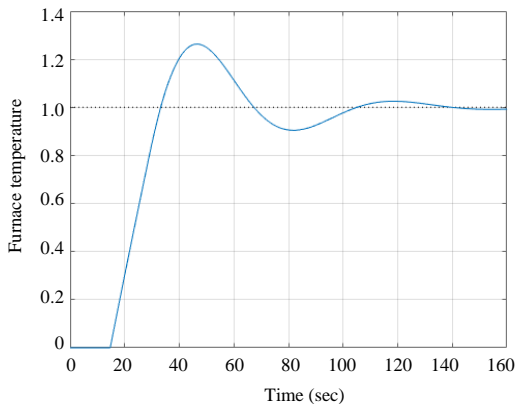


Fig. 13: Furnace temperature

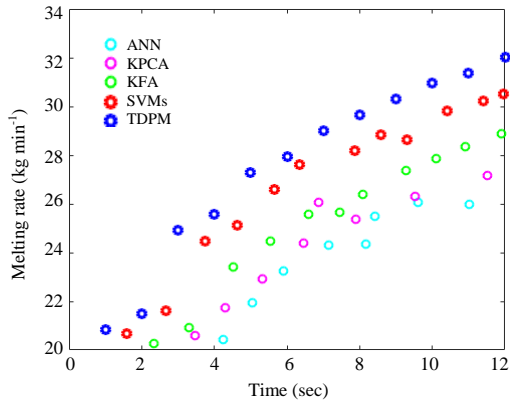


Fig. 14: Scatter diagram comparison

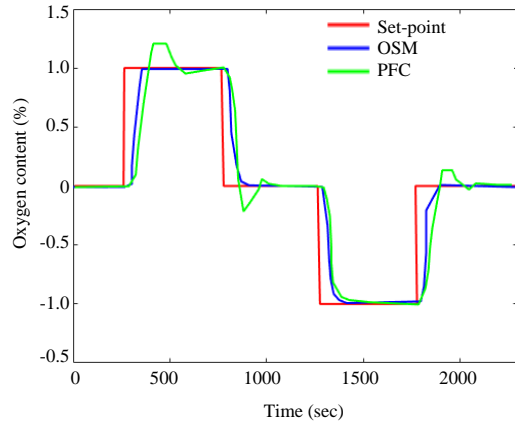


Fig. 16: Comparison of proposed oxygen content

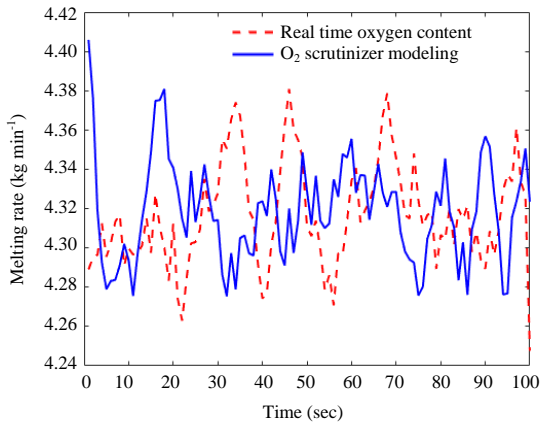


Fig. 15: Comparison with the proposed model

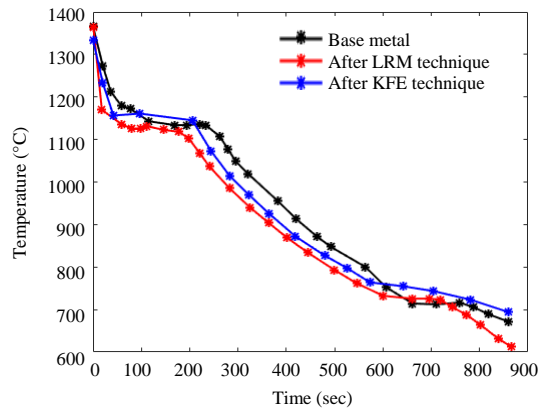


Fig. 17: Comparison with the proposed technique

Figure 14 states the comparison for the proposed Thaw-degree perusal model by analyzing the melting rate. It states that when compared with the existing technologies such as Artificial Neural Network (ANN), Kernel Principal Component Analysis (KPCA), Support vector machine and Kernel Fisher Discriminant Analysis (KFA). Thus, the proposed technique shows the improved performance for the melting rate.

Figure 15 states that the O₂-Scrubtizer model regulates the oxygen content in the cupola furnace. It compares the oxygen content with real-time modeling.

Figure 16 states that O₂-Scrubtizer the model regulate the oxygen content in the cupola furnace. It compares the oxygen content with the existing model, Predictive Functional Control (PFC) to shows our proposed model highly regulates the oxygen content in the furnace.

Figure 17 states the comparison for Kiln Flicker Espial Technique with the existing Logistic Regression Model (LRM). It monitors the performance of the temperature and the stability of the furnace.

CONCLUSION

Cupola furnace is one of the furnaces which melt various types of metal, some of which are cast iron, perhaps bronze. Major issues, that occur during the working of cupola furnaces such as melting process and productivity loss. These issues are efficiently reduced by the novel incinerator-melt enhancement framework which concerns the challenges in the melting process and productivity loss. Along with this Thaw-the degree perusal model improves the melting performance. Also implement the O₂-Scrubtizer model it regulates the oxygen content in the cupola furnace and to handle fluctuations, Kiln Flicker Espial technique which judges the stability of the furnace. The group imbalance problems have a broad advantage and the highest rate of identification fluctuations compared to other approaches. Thus our proposed work utilizes for analyzing the melting rate and competently improves the melting performance and efficiently reduces the productivity loss.

REFERENCES

01. Elorz, J.A.P.S., D.F. Gonzalez and L.F. Verdeja, 2018. Fundamentals of the Cupola Furnace: Applications-Mass and Energy Balances. In: Physical Metallurgy of Cast Irons, Elorz, J.A.P.S., D.F. Gonzalez and L.F. Verdeja (Eds.), Springer, Berlin, Germany, pp: 313-333.
02. Nieto-Delgado, C., F.S. Cannon, P.D. Paulsen, J.C. Furness, R.C. Voigt and J.R. Pagnotti, 2014. Binded anthracite briquettes as fuel alternative to metallurgical coke: Full scale performance in cupola furnaces. *Fuel*, 121: 39-47.
03. Alabi, S.A. and J.O. Afolayan, 2013. Investigation on the potentials of cupola furnace slag in concrete. *Int. J. Integr. Eng.*, Vol. 5,
04. Huang, H., J.T. Fox, F.S. Cannon, S. Komarneni, J. Kulik and J. Furness, 2011. Binding waste anthracite fines with Si-containing materials as an alternative fuel for foundry cupola furnaces. *Environ. Sci. Technol.*, 45: 3062-3068.
05. Aristizabal, R.E., P.A. Perez, S. Katz and M.E. Bauer, 2014. Studies of a quenched cupola. *Int. J. Metalcast.*, 8: 13-22.
06. Gantiez, C., L. Sanchez and B. Obert, 2014. ORC module on a cupola furnace. Proceedings of ECOS 27th International Conference on Efficiency, Cost, Optimization, Simulation and Environmental Impact of Energy Systems, June 15-19, 2014, Turku, Finland, pp: 1-10.
07. Niehoff, T., P. Kokas and A.G. Linde, 2011. Melting starting material in a cupola furnace. U.S. Patent 8,071,013, IFI CLAIMS Patent Services, USA.
08. Arum, C. and G.O. Mark, 2014. Partial replacement of portland cement by granulated cupola slag-sustainable option for concrete of low permeability. *Civil Environ. Res.*, 6: 17-26.
09. Hassan, Z., 2012. Extensive investigations towards the development of a cupola furnace process model: A case study on the cupola furnace operations of Volvo Group Trucks Operations in Skovde, Sweden. Master Thesis, KTH Royal Institute of Technology, Stockholm, Sweden.
10. Balaraman, R. and S.A. Ligorla, 2015. Utilization of cupola slag in concrete as fine and coarse aggregate. *Int. J. Civil Eng. Technol.*, 8: 6-14.
11. Madanhire, I. and C. Mbohwa, 2015. Enhancing maintenance practices at a casting foundry: Case study. University of Johannesburg, Johannesburg, South Africa.
12. Matyukhin, V.I., V.B. Babanin, M.V. Zorin, S.G. Stakheev and A.V. Matyukhina, 2015. Selecting the properties of metallurgical coke for cupola furnaces. *Coke Chem.*, 58: 96-100.
13. Sanket, P. and M. Thomas, 2018. Experimental study on mechanical properties of hardened concrete using cupola slag as partial replacement of cement and coarse aggregate. *Int. J. Res.*, 5: 2046-2052.
14. Isnugroho, K. and D.C. Birawidha, 2018. The production of pig iron from crushing plant waste using hot blast cupola. *Alexandria Eng. J.*, 57: 427-433.
15. Li, J., L. Zhang, G. Zhao and D. Cang, 2018. Pilot Trial of Direct Modification of Molten Blast Furnace Slag and Production of High Acidity Coefficient Slag Wool Fibers. In: Characterization of Minerals, Metals and Materials 2018, Bowen, L. J. Li, S. Ikhmayies, M. Zhang and Y.E. Kalay (Eds.). Springer, Cham, Switzerland, pp: 113-120.
16. Nurjaman, F., A. Shofi, W. Astuti and B. Suharno, 2018. [Making NPI (5-8%Ni) using hot blast cupola furnace with a capacity of 3 tons/day (In Indonesian)]. *J. Mineral Coal Technol.*, 14: 19-29.
17. Pribulova, A., D. Baricova, P. Futas, M. Pokusova and S. Eperjesi, 2019. Cupola furnace slag: Its origin, properties and utilization. *Int. J. Metalcast.*, 13: 627-640.
18. Gabra, M.H., R.K. Jain and A. Tiwari, 2017. Energy efficient cupola furnace via hybridization with a biomass gasifier. *Int. J. Emerg. Technol. Eng. Res.*, 5: 54-62.
19. Kavousi-Fard, A., W. Su, T. Jin, A.S. Al-Sumaiti, H. Samet and A. Khosravi, 2018. A predictive KH-based model to enhance the performance of industrial electric arc furnaces. *IEEE. Trans. Ind. Electron.*, 66: 7976-7985.
20. Meier, T., K. Gandt, T. Hay and T. Echterhof, 2018. Process modeling and simulation of the radiation in the electric arc furnace. *Steel Res. Int.*, Vol. 89, No. 4. 10.1002/srin.201700487
21. Elkoumy, M.M., A.M. Fathy, G.M. Megahed, I. El-Mahallawi, H. Ahmed and M. El-Anwar, 2019. Empirical model for predicting process parameters during electric arc furnace refining stage based on real measurements. *Steel Res. Int.*, Vol. 90, No. 11. 10.1002/srin.201900208